Simultaneous inversion of velocity and Q using wave-equation migration analysis

Yi Shen

ABSTRACT

I develop a method for simultaneous inversion of velocity and Q models. This method poses the simultaneous estimation problem as an optimization problem that seeks optimum velocity and Q models by minimizing user-defined image residuals. Numerical tests on a modified SEAM model with two gas clouds demonstrates the necessity of using such simultaneous inversion, when the existent velocity and Q models are inaccurate. The results show that this simultaneous inversion method is able to retrieve both velocity and Q models, as well as correct and compensate the distorted migrated image caused by inaccurate velocities and Q models.

INTRODUCTION

Because strong attenuation and low-velocity anomalies are present in gas pockets or clouds, they present notoriously challenging problems for reservoir identification and interpretation (Billette and Brandsberg-Dahl, 2005). Attenuation degrades the seismic image quality by damping the image amplitude, lowering the image resolution, distorting the phase of events, and dispersing the velocity. A wrong velocity estimation for the low-velocity anomalies also results in imaging problems, such as mis-positioning of events and discontinuity of the imaged structures. These problems impede accurate image interpretation for hydrocarbon production and well positioning. To mitigate the effects of such gas accumulations on the image and improve imaging of the subsurface, it is important to understand the properties of these gas pockets or clouds. Compressional velocity (V) and compressional quality factor (Q) play an important role in correcting and compensating for the gas-induced distortion in the image.

Shen et al. (2013, 2014) developed a method, wave-equation migration Q analysis (WEMQA), to produce a reliable Q model. This method analyzes attenuation effects from the image space, and uses wave-equation Q tomography to estimate Q models. However, this method requires highly accurate velocity models. An inaccurate velocity model used by WEMQA easily distorts the spectra of the migrated events and causes errors in spectral analysis for estimating the attenuation effects. Therefore, it is necessary to invert for both velocity and Q models if neither of these models is correct. Thus, such an inversion compensates for the errors in Q estimation caused by inaccurate velocities.

In this paper, I initially develop a method for simultaneous inversion of velocity and Q models based on the previous workflow of WEMQA (Shen et al., 2013, 2014). Then I test this method on a synthetic dataset to demonstrate its benefit and effectiveness.

THEORY

I pose the simultaneous estimation problem as an optimization problem that seeks optimum velocity and Q models by minimizing user-defined image residuals:

$$J = J_v(v, Q) + \beta J_Q(v, Q), \tag{1}$$

where β is a weighting parameter that balances two user-defined image residuals $J_v(v, Q)$ and $J_Q(v, Q)$, and can be changed through iterations. The image residuals $J_v(v, Q)$ and $J_Q(v, Q)$ are functions of the current velocity and Q models. However, $J_v(v, Q)$ emphasizes more on the kinematic changes in an image caused by an inaccurate velocity model, while $J_Q(v, Q)$ emphasizes more on the amplitude spectral change in an image caused by an inaccurate Q model.

I use the normalized differential semblance optimization (DSO) (Tang, 2011) as the criterion to mainly estimate the velocity. This objective function normalizes the square of the root-mean-squared (RMS) image amplitudes to reduce the influence of image amplitude variations caused by attenuation and uneven illumination. The normalized DSO objective function is in the subsurface-offset $\mathbf{h}$ domain:

$$J_v = \frac{1}{2} \sum_{\mathbf{x}} \frac{\sum_{\mathbf{h}} |\mathbf{h}|^2 \left| m\left(\mathbf{x}, \mathbf{h}\right)\right|^2}{\sum_{\mathbf{h}} \left| m\left(\mathbf{x}, \mathbf{h}\right)\right|^2}, \tag{2}$$

where $m\left(\mathbf{x}, \mathbf{h}\right)$ is the migrated image with the current velocity and Q models in the subsurface-offset domain. The physical interpretation of the subsurface-offset-domain DSO is that it optimizes the models by penalizing energy at non-zero subsurface offset, taking advantage of the fact that seismic events should focus at zero-subsurface offset if migrated using accurate models.

By definition for J_Q, the image residual primarily coming from attenuation is the difference between the background image computed with the current background models and the attenuation-free image. In fact, instead of computing the difference between these two images, I calculate the spectral change of the images:

$$J_Q = \sum_{\mathbf{x}} \left|\rho\left(\mathbf{x}\right)\right|^2. \tag{3}$$

The change in the spectrum can be indicated by the steepness of the slope $\rho(\mathbf{x})$ computed by the spectral ratio method (Tonn, 1991), between a number of selected, windowed events in the background image and those in the reference windows. These reference windows are carefully selected from the background image to not be contaminated by attenuation. All the windows in this method are large and have the same size; therefore, the influence of the interfering reflectivities on the spectra are statistically the same over all windows. Based on the assumption that the amplitude spectra have the same frequency content over the windows if the models used for imaging are accurate, this method minimizes the spectral differences between the selected windows and the reference windows.

These user-defined residuals are mapped to the perturbations in the current velocity and Q models by the wave-equation velocity and Q tomography operators (Tang, 2011; Shen et al., 2013, 2014). I use the mapped perturbation as gradient directions to conduct a line-search in optimization schemes, to obtain both velocity and Q models.

NUMERICAL EXAMPLE

To demonstrate this methodology, I use a portion of the SEAM synthetic velocity, adding two gas clouds with lower velocity than the surrounding sediments, as shown in Figure 1(a). The Q model (in logarithmic scale) shown in Figure 1(b) also includes these two gas clouds with high attenuation. I generate a 2D synthetic data with 56 shots with 100 m spacing, 137 receivers with 40 m spacing, and a Ricker source wavelet with 12 Hz central frequency.

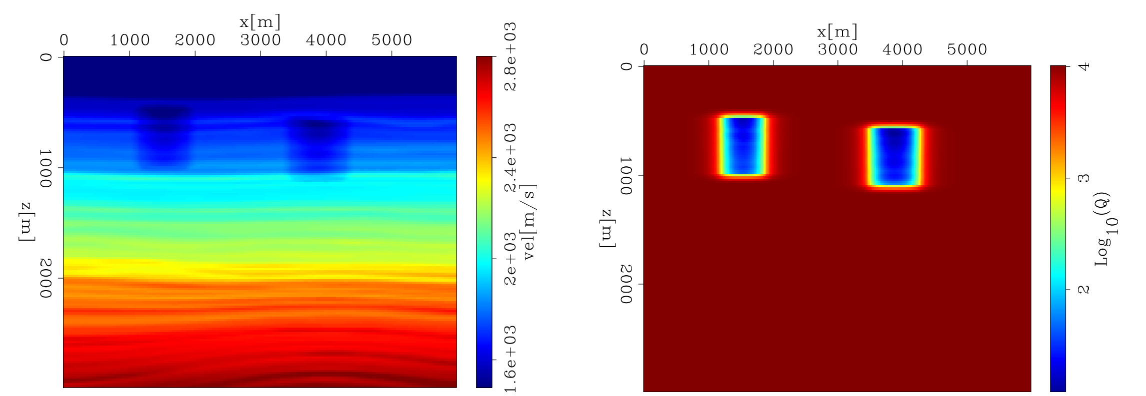

(a) (b)

Figure 1: True models: (a) A part of a modified SEAM velocity model with two gas clouds; (b) Q model (in logarithmic scale) with two gas clouds. [**CR**]

The first test in this example is to invert for the Q model with the inaccurate velocity model shown in Figure 2(a). The inaccurate velocity in Figure 2(a) has the same background velocity as that in Figure 1(a). However, the velocity of the left gas cloud in Figure 2(a) is slightly higher than the true velocity in Figure 1(a) and is set to be the same as the surrounding sediments; while the velocity of the right gas cloud in Figure 2(a) remains unchanged from the true velocity in Figure 1(a).

The initial model for Q inversion is a model without attenuation. Figure 2(b) shows the inversion results (in logarithmic scale) using WEMQA (Shen et al., 2013, 2014). The results show that this Q inversion method with adequately accurate velocity information of the right part of the model, as shown in Figure 2(a), sufficiently recovers the location and value of the right gas cloud, as shown in Figure 2(b). However, this method with inaccurate velocity in the left part of the model, as shown in Figure 2(a), fails in retrieving the left gas cloud. The main reason for this failure is the inaccurate velocity that distorts the kinematics of the migrated structures, and subsequently degrades the accuracy of the spectra analysis for Q inversion. Therefore, simultaneous inversion of both velocity and Q models is needed to obtain a reasonable inversion results, if accurate information of these models is not available.

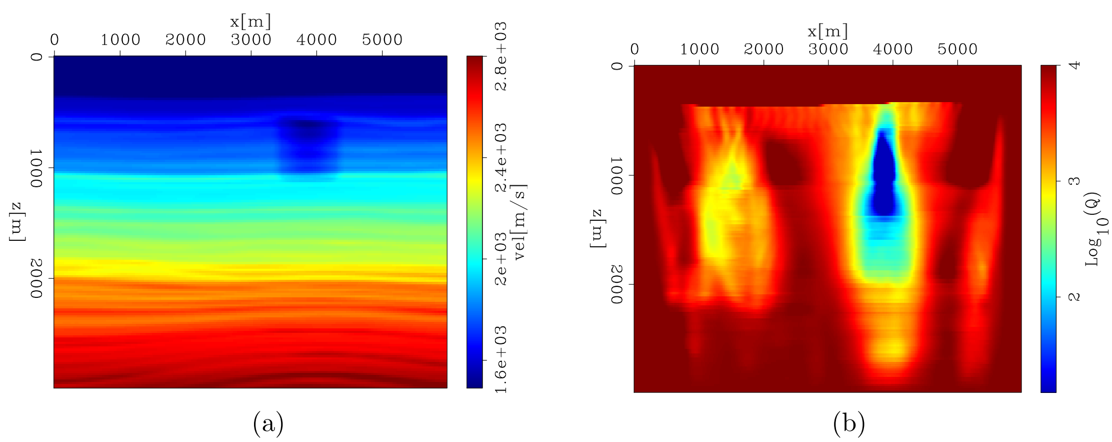

Figure 2: (a) Inaccurate initial velocity model for Q inversion with only one gas cloud instead of two. Initial Q is constant. (b) Inverted Q model using inaccurate velocity model in Figure 2(a). [**CR**]

To simultaneously invert for velocity and Q models, the initial velocity model has the same background velocity and right gas velocity, as shown in Figure 1(a), but without the velocity drop in the left gas cloud. The initial Q model is a model without attenuation. Figure 3(a) is the inverted velocity model and Figure 3(b) is the inverted Q model. Simultaneous inversion successfully retrieves the locations and values of both gas clouds in velocity and Q models, as shown in Figure 3.

Figure 4(a) is the migrated image using the initial velocity and Q models. The initial velocity model has a larger velocity in the left gas cloud, which causes the events below to be pushed downward and discontinuous. Attenuation caused by these two gas clouds degrades the quality of the deep imaged structures in Figure 4(a), in terms of dimming the amplitudes, making the events incoherent and stretching the wavelets. Figure 4(b) is the migrated image using the inverted models in Figure 3. Migration with the improved velocity model in Figure 3(a) moves the events below the left gas cloud upward and makes the events there more coherent. Also, compensation with the

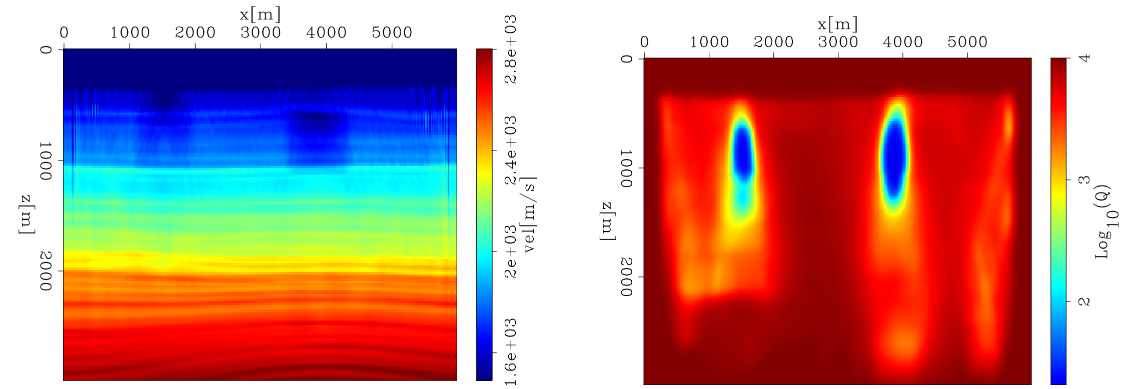

(a) (b)

Figure 3: Simultaneous inversion results: (a) The inverted velocity model. Note how the gas cloud on the left has been recovered. (b) The inverted Q model. The Q value of the left gas cloud has been recovered. [**CR**]

inverted Q model shown in Figure 3(b) makes the events sharper and more balanced in both phase and amplitudes, as shown in Figure 4(b).

Figure 5(a) and Figure 5(b) are the angle domain common image gathers(ADCIG) extracted from the left gas cloud location (x= 1500 m) and obtained with the initial models and the inverted models in Figure 3, respectively. The inaccurate large velocity causes the events to be unflattened, as shown in Figure 5(a). The inverted velocity model shown in Figure 3(a) corrects such kinematics error caused by such wrong velocity and flattens the events in Figure 5(b). In addition, migration with the inverted Q model in Figure 3(b) compensates for the energy loss that appears especially strong at the near angle as shown in Figure 5(a), and therefore makes the amplitude of the events more balanced in Figure 5(b).

Figure 6(a) and Figure 6(b) are the angle domain common image gathers(ADCIG) extracted from the right gas cloud location (x= 3800 m) and obtained with the initial models and the inverted models in Figure 3, respectively. The near angles in Figure 6(a) have low amplitudes, stretched wavelets and unflattend events caused by attenuation, although the velocity used in this region is correct. Imaging with the inverted Q model in Figure 3(b) compensates the high frequency loss caused by attenuation, therefore, it recovers the amplitudes and sharpens the events at the near angles in Figure 6(b). In addition, such compensation corrects the phase distortion and velocity dispersion caused by attenuation. Subsequently, the events in Figure 6(b) become more flattened and more coherent than the events in Figure 6(a).

CONCLUSION

I developed a method for simultaneous inversion of velocity and Q models. This method poses the simultaneous estimation problem as an optimization problem that

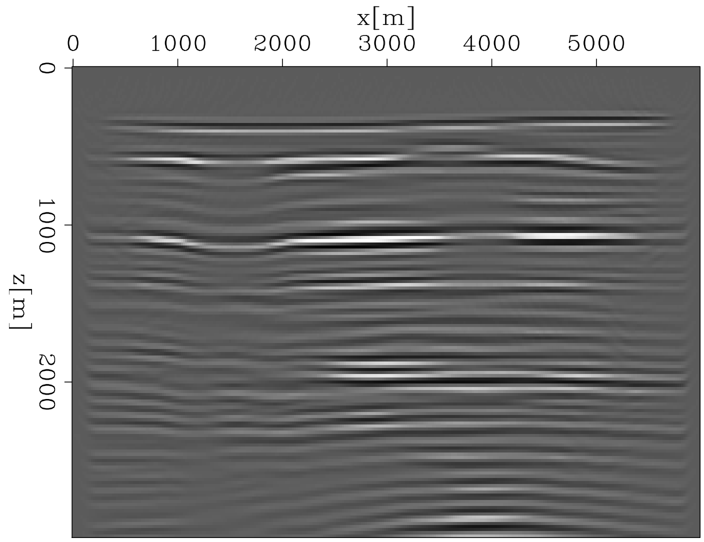

(a)

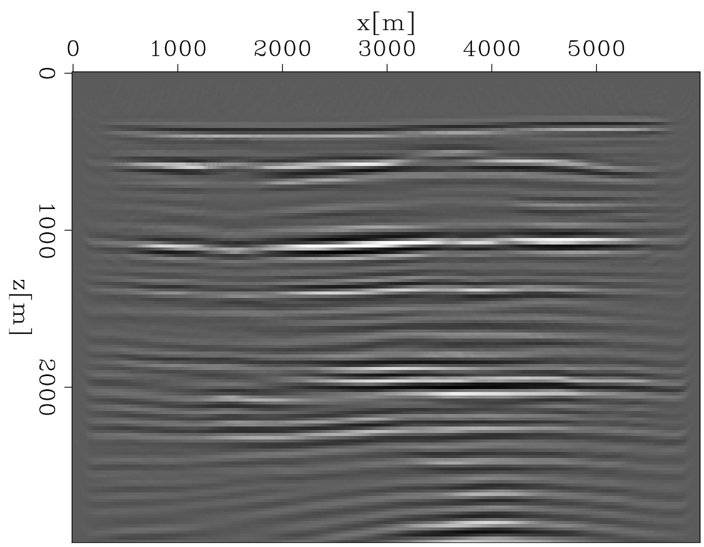

(b)

Figure 4: (a) The migrated image using the initial velocity and Q models; (b)The migrated image using the inverted models in Figure 3. The kinematics and the amplitudes under the gas cloud are corrected for by the inverted model. [**CR**]

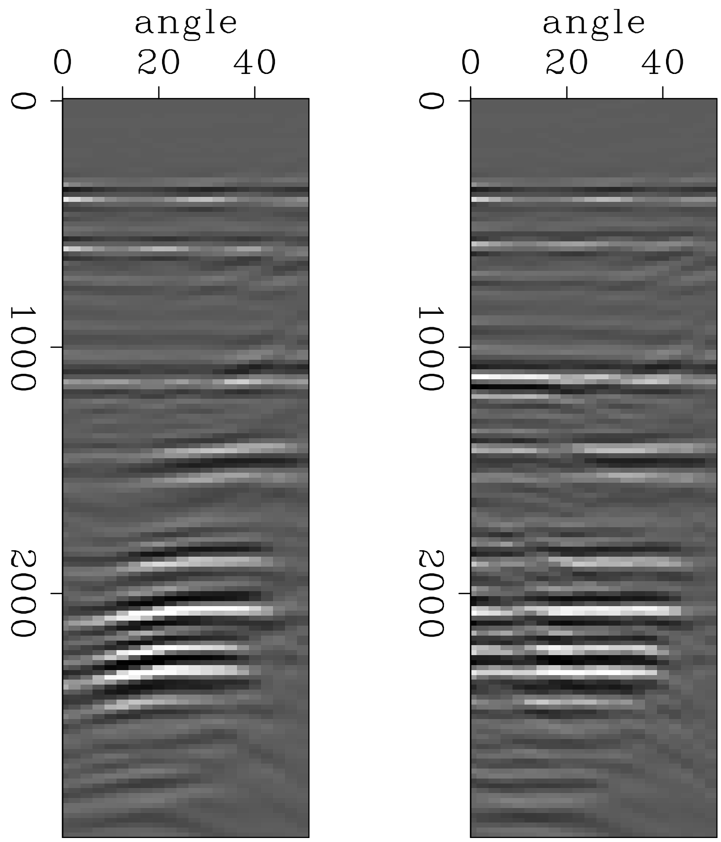

(a) (b)

Figure 5: (a)The angle domain common image gathers(ADCIG) extracted from the left gas cloud location (x= 1500 m) and obtained with the initial models. The vertical axis is depth with unit of meter. (b) The angle domain common image gather(ADCIG) extracted from the left gas cloud location (x= 1500 m) and obtained with the inverted models shown in Figure 3. The vertical axis is depth with unit of meter. The events are flattened, and the low angle amplitudes have been recovered. [**CR**]

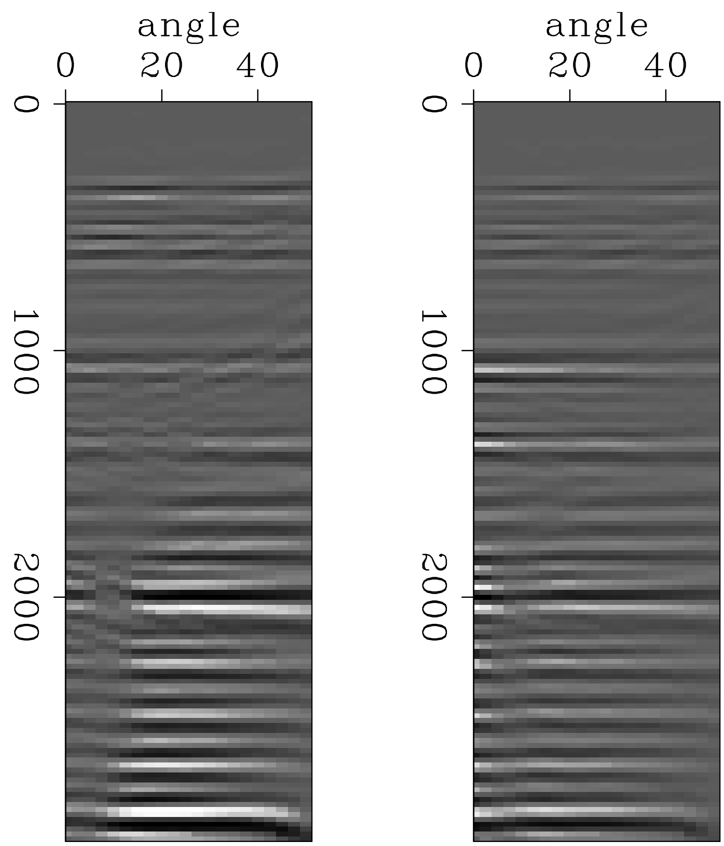

(a) (b)

Figure 6: (a)The angle domain common image gathers(ADCIG) extracted from the right gas cloud location (x= 3800 m) and obtained with the initial models. The vertical axis is depth with unit of meter. (b) The angle domain common image gather(ADCIG) extracted from the right gas cloud location (x= 3800 m) and obtained with the inverted models in Figure 3. The vertical axis is depth with unit of meter. Imaging with the inverted Q model recovers the amplitudes and sharpens the events at the near angles. Such compensation also corrects the phase distortion and velocity dispersion caused by attenuation, which makes the events more flattened and more coherent. [**CR**]

seeks optimum velocity and Q models by minimizing user-defined image residuals. The numerical tests on a modified SEAM model with two gas clouds demonstrate the benefit of using such simultaneous inversion, when the existing velocity and Q models are inaccurate. The results show that this simultaneous inversion method is able to retrieve both velocity and Q models, and to correct and compensate the distorted migrated image caused by inaccurate velocity and Q models.

ACKNOWLEDGMENTS

The author thanks Biondo Biondi and Robert Clapp, from the Stanford Exploration Project, for their advice and suggestions. Special thanks to Yunyue Li, Yang Zhang and Guillaume Barnier for their fruitful discussions.

REFERENCES

Billette, F. and S. Brandsberg-Dahl, 2005, The 2004 BP velocity benchmark: 67th Conference and Exhibition, EAGE, Extended Abstracts, B035.

Shen, Y., B. Biondi, R. Clapp, and D. Nichols, 2013, Wave-equation migration Q analysis (WEMQA): EAGE Workshop on Seismic Attenuation Extended Abstract O22.

——, 2014, Wave-equation migration Q analysis (WEMQA): SEG Technical Program Expanded Abstracts.

Tang, Y., 2011, Imaging and velocity analysis by target-oriented wavefield inversion: PhD thesis, Stanford University.

Tonn, R., 1991, The determination of seismic quality factor Q from VSP data: A comparison of different computational techniques: Geophysical Prospecting, **45**, 87–109.